International Journal of Electrical and Computer Engineering (IJECE)
Vol. 12, No. 5, October 2022, pp. 4623~4631
ISSN: 2088-8708, DOI: 10.11591/ijece.v12i5.pp4623-4631

Impacts of integration of wind farms on voltage stability margin

Hani Attar[1], Mehrdad Ahmadi Kamarposhti[2], Ahmed Amin Ahmed Solyman[3]
[1]Department of Energy Engineering, Zarqa University, Zarqa, Jordan
[2]Department of Electrical Engineering, Jouybar Branch, Islamic Azad University, Jouybar, Iran
[3]Department of Electrical and Electronics Engineering, Faculty of Engineering and Architecture, Nisantası University, Istanbul, Turkey

Article Info

Article history:

Received Sep 15, 2021
Revised May 21, 2022
Accepted Jun 6, 2022

Keywords:

Doubly-fed induction generator
Power system
Voltage stability margin
Wind farm

ABSTRACT

The current methods use conservative voltage based on the maximum wind speed with simultaneous occurrence in peak loading conditions to determine the maximum size of the wind farm. Wind patterns never let the wind farm on the wind farm site produce its maximum capacity during hours of heavy loading conditions. A new method is presented in this research to determine the maximum size of wind farms including voltage stability margin (VSM) and wind patterns at the wind farm site in the size of a wind farm. This plan is a method to increase the maximum size of a wind farm with a limited wind generation option under certain conditions based on VSM. The proposed method is applied to the wind farm in the IEEE 14-bus network power system. The results of the new method show that the maximum size of wind farms increases when the system operates with intermittent wind control to maintain the voltage stability.

Corresponding Author:

Mehrdad Ahmadi Kamarposhti
Department of Electrical Engineering, Jouybar Branch, Islamic Azad University
Jouybar, Iran
Emails: mehrdad.ahmadi.k@gmail.com, mehrdad.ahmadi@iau.ac.ir

1. INTRODUCTION

Integration of renewable power generation on electricity grid has been increasing significantly due to some benefits of abundant sources and environmental issues. Moreover, the development of energy conversion and material technologies encourages integration of renewable energy resources-based power plants on power system network. Despites the advantages of integrating novel power plant technologies, the increasing penetration of renewable power plant introduces some challenges on power system operation. Integration of large-scale renewable energy-based power plant significantly affects power flow and stability of interconnected power system network. The increase of intermittency and uncertainty in power system as a consequence of integrating renewable energy would affect the equilibrium point of power system operations. The balance conditions dynamically change due to unpredictable power contribution from renewable energy based power generation [1].

It has been shown in various references that increasing wind permeability increases demand for more radioactive power. If it is not supplied by the existed power system, it may lead to voltage instability [2], [3]. Voltage stability constraints have become the most limiting factor against the increase of wind generation permeability in power systems by increasing wind production permeability in power systems and their reactive power demand [3], [4].

The maximum level of wind force permeability depends on the available voltage stability margin (VSM) of the existing power system [5], [6]. New wind farms with a less negative effect on VSM must have a bigger size to maximize the level of wind permeability in a power system. As a result, limiting the maximum size of wind farms may not maximize the level of wind permeability based on the assumption that high wind speeds occur at peak loading conditions simultaneously [6].

In study [7], wind farms are measured based on the maximum size of the wind farm due to their effect on VSMs. Wind farms with the minimum negative effect on VSMs are larger than other farms. It was assumed in calculating the maximum voltage stability of the wind farm size that wind sources would also be available during peak load hours to generate electricity with peak load simultaneously. Although this approach provides stable voltage for wind farm size at any conditions, it is very conservative.

The wind farm size can be increased higher than the maximum size by considering the actual levels of wind speed at peak loading conditions [7]. Wind production is limited under certain conditions based on VSM with this option. The wind power output in this research tends to be maximum during the early morning hours and at night and be minimum during the afternoon hours when the loads in the region are at their peak [6]–[35].

This paper is a new practical approach to evaluate the effect of wind permeability increase by combining VSMs system, loading pattern, and existed wind resources in wind generation sites. The rest of this paper is organized. In section 2, voltage stability problem is described. Wind injection point and load modeling introduced in section 3. In section 4, evaluating voltage stability is presented. In section 5, the problem formulation is given. In section 6, the understudy power system is presented then the simulation results are analyzed. Finally, this article concludes in section 7.

2. VOLTAGE STABILITY MARGIN

Voltage stability is described by the slow reduction of voltage levels in one or more buses in a power system. Static and dynamic methods can be used to investigate voltage stability constraints. Since voltage decays slowly in many cases, voltage stability can be effectively analyzed by a static approach instead of a dynamic approach. Steady-state voltage stability analysis lets system programmers use steady-state load distribution models easily for voltage stability studies.

VSM can be calculated at any functional point of the system with high reliability when production resources are available to supply load demand. Nonetheless, VSM is calculated more complicatedly at any given time due to the nature of wind generators and their unpredictable output power as generation sources change to accommodate new wind power units and supply load demand. Using the expected voltage stability margin (EVSM) index has been studied in voltage stability analysis of power systems under various system configurations and load conditions [35]. EVSM can be used to measure the stability voltage of a system with unpredictable production sources such as wind generation.

3. WIND INJECTION POINT AND LOAD MODELING

In recent years, the doubly-fed induction generator (DFIG) type has become more popular than the SCIG type because of its ability to consume or produce reactive power according to the lack of reactive power support in areas with the installed wind farms. The DFIG wind generator can change its functional speed to get optimal wind power extraction. This issue is solved by feeding the rotor circuit with active and reactive power from the rotor side converter. The lateral converter is connected between the rotor circuit and the power system and is usually measured for a part of the generator specification plate [2]. Only wind farm DFIG is studied in this research.

Power system loads are voltage sensitive and their response to voltage fluctuations at each step of voltage stability calculation should be modeled for power systems. The load dynamics would have a significant effect on the breakdown point calculations even for slow voltage breakdowns whenever the voltage drops below 0.9 p.u in a load bus. The voltage limit of 0.9 p.u is based on the voltage control of power systems that keep loads constant. However, the load would not be constant anymore when the system voltage level is less than 0.9 p.u [7]. Since it is assumed that all bus-loads are kept at voltages above 0.9 p.u at each stage of VSM calculation, load dynamics are not considered in this research. When the voltage of each bus-load drops below 0.9 p.u or reaches the point of voltage breakdown, the voltage gets unstable in a power system.

4. EVALUATING VOLTAGE STABILITY

The power system experiences a mode of voltage instability when there is a progressive or uncontrollable decrease in voltage level after a failure and an increase in load demand or a change in operating conditions. An increase of reactive power "Q" increases the voltage at bus "V" for a stable voltage system. An increase in reactive power "Q" decreases the voltage at bus "V" for an unstable voltage system [6].

The used Q-V curve method to calculate VSM has many advantages over the other static voltage stability analysis tools. This is particularly when the lack of reactive power "Q" makes power systems arrive at the falling point. No bus voltage should drop below 0.9 p.u according to this research and local instrument criteria. According to Figure 1, VSM is defined as the measured Megawatt distance difference of reactive power from the operating point to the bottom of the Q-V curve (Q_{min}) or from the point where the bus voltage drops below 0.9 (Q 0.90 pu) [5].

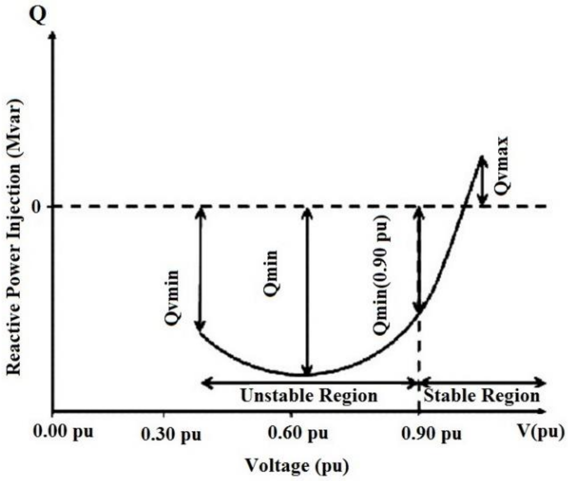

Figure 1. Q-V specification curve [2]

5. EVALUATING THE EXPECTED VOLTAGE STABILITY

The described EVSM in [7] can be used to measure the effect of wind farm size on system voltage stability. EVSM is defined as the sum of VSM of each wind speed multiplied by its probability of occurrence to consider the probabilistic nature of wind speed as shown by (1):

$$EVSM = \sum_{i=1}^{n} VSM(V_{wind}) * probability\ (V_{wind}) \quad (1)$$

in which, V-wind is the calculated VSM in the measured wind speed in wind farm site. "Probability (V_wind)" is the probability of wind speed occurrence, and "n" is the number of different wind speed intervals included in EVSM calculations.

A new expected voltage stability index Li has been introduced to evaluate the effect of increasing wind farm size on voltage stability. The new index provides a quantitative measure of system voltage stability changes to increase wind permeability. The great amount of Li shows that system is closer to change to any instability for all changes in a system parameter such as power coefficient changes and load changes. the lower value of the Li index shows that system is strong, and system instability is not significantly impressed by the change in wind farm size.

Li is calculated by subtracting system final EVSM from the system initial EVSM and dividing by the system initial EVSM. The Li index can be expressed as (2).

$$L_i = \frac{\mathrm{EVSM}_b - \mathrm{EVSM}_a}{\mathrm{EVSM}_b} \quad (2)$$

In which, $EVSM_b$ is the expected voltage stability margin of the system before increasing the wind farm size and $EVSM_a$ is the expected voltage stability margin of the system after increasing the wind farm size. Li index is between 0 and 1. 0 shows that the system expected voltage stability is not impressed by an increase in wind farm size. 1 shows that the expected voltage stability of the system becomes unstable with an increase in wind farm size.

The following part describes the steps of a principled method to evaluate the effect of increasing the wind farm size to values higher than its maximum voltage stability limit. These steps can be used to evaluate the effect of each power system with several wind farms because loading distribution is modified to put all the manufacturing units despite their types before calculating VSM. The following steps describe the new method.

- Step 1: The peak load of the power distribution sample is selected as the base sample before wind injection from the available seasonal load distribution samples. The peak load sample is an example that includes the peak load month.
- Step 2: The wind farm injection site and the type of used wind turbines are specified.
- Step 3: Indicating the connected bus voltage to the wind farms and the power factor at the connection point for the new wind injection site.
- Step 4: identifying the peak month for analysis. Peak month is divided into 24 hours per day in a way that each hour per day is the repetition of 30-31 loads during a peak month depending on which month the peak occurred.
- Step 5: Setting the peak loads in every 24 models made equal to the peak load for each hour of the day.
- Step 6: Selecting an hour of a day for analysis by starting from one hour (12 a.m. and 01:00 a.m.).
- Step 7: Gradual increase of the wind farm size in the load distribution model until the voltage dissipation and obtaining VSM of the maximum wind farm power for each hour load.
- Step 8: Calculating $EVSM_b$ as a function of wind speed for the maximum obtained size in step 7. VSM is calculated for each increase change. Then, it is multiplied by the probability of its output power. The sum of all VSMs in the system is $EVSM_b$.
- Step 9: Increasing the maximum farm wind size in step 7 to obtain a new VSM to calculate $EVSM_a$.
- Step 10: Calculating VSM for each range then multiplying by VSM for each power range of wind farm in its range probability. The sum of all EVSMs for all levels of wind farm output power is the new $EVSM_a$ system for the new wind farm size.
- Step 11: System EVSM calculation is shown by Li index in (2), and calculating the expected outage hour of the wind farm based on the probabilities of wind farm output power.
- Step 12: Repeating steps 6 to 11 for all the remained daily hours, time of 2 to 24.
- Step 13: end

6. RESULTS OF SIMULATION

The suggested wind farm measuring method is applied to the 14-bus IEEE power system which is shown in Figure 2. Two new wind farms in 2 desperate areas have been studied for a 14-bus IEEE power system for the optimum measurements. All 2 wind farms were located in the same class and the internal connection of the same transmission equipment at 13.8 kV.

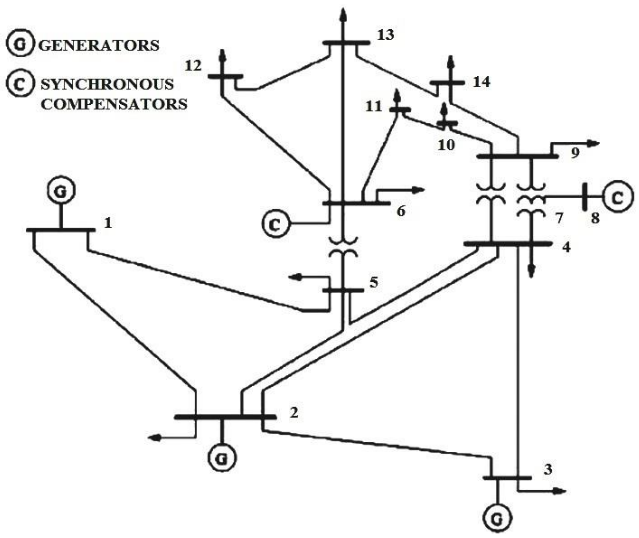

Figure 2. Single-line diagram of the IEEE 14-bus system

The new wind farms are connected to the grid at a voltage of 13.8 kV and are modeled as a PQ bus at the connection point with a constant pre-phase/post-phase power factor of 0.95. The calculated VSM is produced using the mentioned wind power combination. In the mentioned peak month, the load peaked in the afternoon (4-6 p.m.) as shown in Figure 3 in blue. Most irrigation loads are small commercial and residential loads. Wind injection into the basic model reduced VSMs for all hours of the day. The maximum amount of wind injection shown in Figure 3 in red color is the maximum wind farm size that can be safely injected into the system without voltage stability for each hour of the day.

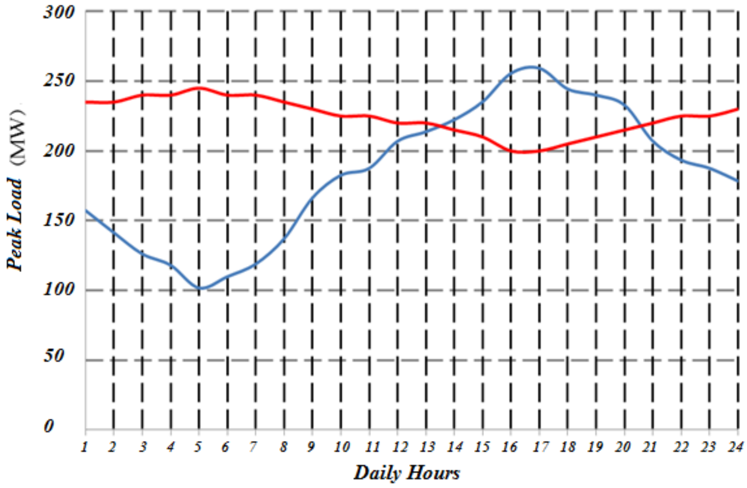

Figure 3. Maximum load of hour peak for peak months and maximum wind farm size for 14-bus IEEE network power system

The maximum wind farm size at this hour of the day is called the stable voltage wind farm size. If the maximum field wind does not exceed 200 MW, there will be no expected wind hours. Days 16 and 17 have led to the lowest maximum level for this wind farm. The maximum size of the wind farm is reached in hours of days 1 to 8. The DFIG wind farm in western Kansas was used to calculate the expected output power at the wind farm site for the entire hour of July, which we implemented on the IEEE 14-bus network power system [8]. At least wind speed hour data of 3 years (2005-2007) and the maximum wind speed were used in three years to calculate hours with the minimum VSMs. The expected wind farm output power and their probability as a percentage of the maximum DFIG specification plate at the wind farm site in West Kansas for the daily hour was used in the 14-bus IEEE power network which is shown in Table 1.

Three new sizes were investigated to study the effect on VSM and EVSM by increasing the wind farm size higher than the voltage stability size of 200 MW. The newly used sizes are in load distribution models of 250 Mw, 300 Mw, 350 Mw, and 400 Mw. As it is seen in Table 2, the increase in the number of outage hours may not lead to the significant change between samples 4 and 5. Because many expected work hours of wind farm are classified in 90% to 100% of the wind farm *specification plate* or around 0% to 10% of the *specification plate*. In agreement with the reference [4], it shows that the power of wind farms is mainly utilized at their maximum level, near the maximum output, at their minimum level, or near their minimum based on their wind speed relationship.

Table 1. The expected wind farm output power and their probability as a percentage of the maximum DFIG specification plate at the wind farm site

Probability of wind output power from DFIG wind farm in western Kansas		
Probability	Daily hour of peak month	
	No. of observation hours	% of power
0.193548387	6	0.00%
0.032258065	1	10.00%
0.064516129	2	20.00%
0.032258065	1	30.00%
0.064516129	2	40.00%
0.032258065	1	50.00%
0.032258065	1	60.00%
0.032258065	1	70.00%
0.096774195	3	80.00%
0.193548387	6	90.00% - 95.00%
0.225806452	7	96.00% - 100.00%
1.000000000	31	Total

Table 2. A summary of the effect of wind farm size increase on the system EVSM and the outage expected hour for the peak month

	Modes	Daily hours Peak load	16 255.65	17 259.29	Total expected outage hours	Mean EVSM for daily hours (Mvar)
Maximum power output in the 14-bus IEEE system	Mode 1 200 Mw	outage hour $EVSM_a$	0 24.62	0 24.55	0	24.58
	Mode 2 250 Mw	outage hour $EVSM_a$	7 15.19	7 15.15	14	15.17
	Mode 3 300 Mw	outage hour $EVSM_a$	16 12.32	16 12.29	32	12.30
	Mode 4 350 Mw	outage hour $EVSM_a$	17 11.74	17 11.43	34	11.58
	Mode 5 400 Mw	outage hour $EVSM_a$	18 11.24	18 11.21	36	11.22

EVSM Li index was calculated for maximum size of the increased wind farm. The Li index increases by the field wind increases. This indicates that VSM of the system decreases as more wind is injected into the system. The maximum Li was found in sample 5 at daily 17 o'clock. During this daily hour, the system is at its minimum point of stability. EVSM Li index changes much less between samples 3 and 4 than between samples 2, 3 and 4.

This shows that increasing the system wind farm size to higher than 200 Mw reduces voltage stability. 400 Mw wind farm produced the maximum Li index that the worst mode is analyzed among 5 samples. The mean Li index for the 400 MW sample reached 0.534, which is 40.1 times higher than the calculated mean Li index for the 250 MW sample (sample 2). Table 3 shows the effect of the maximum increase of wind farm size on the system's expected voltage stability. Notice that $EVSM_a$ does not predict the daily hour with the worst stability while combining the wins speed patterns in their calculation values. In sample 5, the worst EVSM for the daily hour of 17 o'clock was calculate 11.22 Mvar with EVSM of Li index of 0.534 that was the worst value for all the studied cases. The outage hours were determined higher than 200 Mw by counting the hours of wind farm production. Figure 4 shows the summary of Table 3.

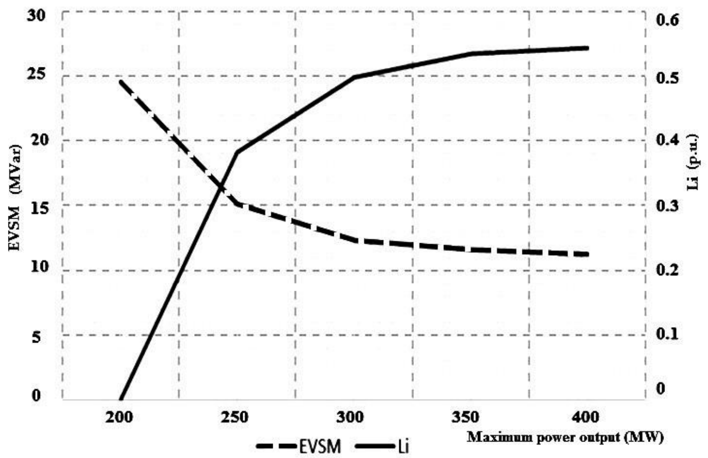

Figure 4. The mean EVSMs and Li index at 16 and 17 o'clock

It is assumed that a control scheme inside the wind farm could be to an outage of wind turbines to reduce wind farm output power during peak hours. A special protection design is a form of control design that can be used to reduce voltage collapse in the system because of an increase in wind farm size to higher than its maximum voltage.

The expected number of outage hours increases when the maximum wind farm size increases. Increasing the wind farm size from 200 to 250 MW will result in 14 hours outage. The outage time has more than doubled with a further increase in wind farm size. The potential outage hour has increased to 34 and 36 in modes 4 and 5 because system VSM reduced for wind injection. It is expected that the outage hour occurs when the output power of the wind farm is higher than 57% of the specification plate for a sample of 350 Mw and higher than 50% of the specification plate for a sample of 400 Mw.

Table 3. The expected voltage stability index, Li, for the maximum changes of wind farm size

Peak month	Daily hours	16	17	Mean
Model 1	EVSM	24.62	24.55	24.58
200 MW				
Mode 2	EVSM	15.19	15.15	15.17
250 MW	Li	0.383	0.382	0.3825
Model 3	EVSM	12.32	12.29	12.30
300 MW	Li	0.499	0.499	0.499
Mode 4	EVSM	11.74	11.43	11.58
350 MW	Li	0.534	0.534	0.534
Mode 5	EVSM	11.24	11.21	11.22
400 MW	Li	0.543	0.543	0.543

7. CONCLUSION

It was shown that increasing wind farm size higher than voltage stability size limit can increase the wind permeability. However, the maximum wind farm output power may be limited to protect the power system against voltage collapse because of wind speed patterns and the availability of reactive power. In addition, the obtained results from the analysis showed that system EVSMs reduce as to increase wind farm size. Wind farms that are sized above voltage stability value experience an increase in the outage hour by system EVSMs reduction. Increasing the wind farm size from 200 to 400 MW reduces the mean EVSM by 35.54%. Higher instability risk and higher the number of outage hours are expected to lower the EVSM value. The decrease in $EVSM_a$ approaches the system operating to the point of voltage breakdown. Increasing the wind farm size too high in some cases and at a certain size, the level increases the minimum wind power permeability due to high outage hours of wind farm output power. The presented method in this chapter is recommended to determine the effect of maximum wind farm size increase over the voltage stability size. This method can be used for proper evaluation. If the size increases, more wind energy is injected. In addition, wind speed patterns are combined to study the effect on the system VSM. If the power system acts at low EVSM, the number of outage wind hours may be very high. This new approach can be used in any number of wind farms proposed in any power system. Increasing wind permeability negatively influences the other types of stability such as small-signal stability by increasing the maximum wind farm size higher than the voltage stability limits. The negative effect of instability mode is expected by increasing wind permeability in weak power systems. Using modal analysis is very important for all wind permeability levels to identify where in wind farm has the greatest effect on the instability modes and what maximum size is the wind farm intensified.

REFERENCES

[1] F. Gonzalez-Longatt and J. L. Rueda Torres, "Advanced smart grid functionalities based on powerfactory," in *Green Energy and Technology*, Springer International Publishing, 2018, pp. E1--E1., doi: 10.1007/978-3-319-50532-9_15.
[2] C. W. Taylor, "Power system voltage stability," McGraw-Hill, 1994., doi: 10.1007/978-3-030-44184-5_263.
[3] M. Chinchilla, S. Arnalte, J. C. Burgos, and J. L. Rodríguez, "Power limits of grid-connected modern wind energy systems," *Renewable Energy*, vol. 31, no. 9, pp. 1455–1470, Jul. 2006, doi: 10.1016/j.renene.2004.03.021.
[4] N. T. Linh, "Voltage stability analysis of grids connected wind generators," in *2009 4th IEEE Conference on Industrial Electronics and Applications*, May 2009, pp. 2657–2660., doi: 10.1109/ICIEA.2009.5138689.
[5] G. Coath and M. Al-Dabbagh, "Effect of steady-state wind turbine generator models on power flow convergence and voltage stability limit," *Australasian Universities Power Engineering Conference (AUPEC 2005).*, 2005
[6] Kansas Energy, "Energy information for the southern plains," *Kansas Energy Information Network*. 2009.
[7] Y. Li, H.-D. Chiang, H. Li, Y.-T. Chen, D.-H. Huang, and M. G. Lauby, "Power system load ranking for voltage stability analysis," 2006., doi: 10.1109/PES.2006.1709345.
[8] G. Wi´sniewski, "Determination of the energy potential polish regions in terms of renewable sources of energy-lessons for regional operational programmes for the period 2014-2020 programming evaluation." Ministry of Regional Development: Warsaw, Poland, 2011.
[9] M. Pietrzak, B. Igliński, W. Kujawski, and P. Iwański, "Energy transition in poland—assessment of the renewable energy sector," *Energies*, vol. 14, no. 8, Apr. 2021, doi: 10.3390/en14082046.
[10] P. Beiter, M. Elchinger, and T. Tian, "2016 renewable energy data book," *Central Statistical Office, Renewable Energy*, 2016. Accessed: Jun. 24, 2021. [Online]. Available: https://www.nrel.gov/docs/fy18osti/70231.pdf
[11] IRENA, "Renewable energy statistics 2017," *Central Statistical Office*. Accessed: Jun. 24, 2021. [Online]. Available: https://www.irena.org/-/media/Files/IRENA/Agency/Publication/2017/Jul/IRENA_Renewable_Energy_Statistics_2017.pdf
[12] Marshal's Office of the Podlaskie Voivodeship, "Podlaskie voivodeship development strategy 2020," *Marshal's Office of Podlaskie Voivodeship*. Accessed: May 20, 2021. [Online]. Available: https://strategia.wrotapodlasia.pl/resource/file/download-file/id.459
[13] Ministry of Climate and Environment, "Energy policy of poland until 2024," *Ministry of Climate and Environment*, Ministry of Climate and Environment, Poland, 2021.
[14] P. B. Eriksen, T. Ackermann, H. Abildgaard, P. Smith, W. Winter, and J. M. Rodriguez Garcia, "System operation with high wind penetration," *IEEE Power and Energy Magazine*, vol. 3, no. 6, pp. 65–74, Nov. 2005, doi: 10.1109/MPAE.2005.1524622.
[15] P. R. Nakhi and M. A. Kamarposhti, "Multi objective design of type II fuzzy based power system stabilizer for power system with wind farm turbine considering uncertainty," *International Transactions on Electrical Energy Systems*, vol. 30, no. 4, pp. 1–20,

Apr. 2020, doi: 10.1002/2050-7038.12285.
[16] G. Magdy, G. Shabib, A. A. Elbaset, and Y. Mitani, "A novel coordination scheme of virtual inertia control and digital protection for microgrid dynamic security considering high renewable energy penetration," *IET Renewable Power Generation*, vol. 13, no. 3, pp. 462–474, Feb. 2019, doi: 10.1049/iet-rpg.2018.5513.
[17] F. Blaabjerg, Y. Yang, D. Yang, and X. Wang, "Distributed power-generation systems and protection," *Proceedings of the IEEE*, vol. 105, no. 7, pp. 1311–1331, Jul. 2017, doi: 10.1109/JPROC.2017.2696878.
[18] P. Kundur *et al.*, "Definition and classification of power system stability IEEE/CIGRE joint task force on stability terms and definitions," *IEEE Transactions on Power Systems*, vol. 19, no. 3, pp. 1387–1401, Aug. 2004, doi: 10.1109/TPWRS.2004.825981.
[19] M. Zhou, J. Zhai, G. Li, and J. Ren, "Distributed dispatch approach for bulk AC/DC hybrid systems With high wind power penetration," *IEEE Transactions on Power Systems*, vol. 33, no. 3, pp. 3325–3336, May 2018, doi: 10.1109/TPWRS.2017.2762358.
[20] F. Blaabjerg, R. Teodorescu, M. Liserre, and A. V Timbus, "Overview of control and grid synchronization for distributed power generation systems," *IEEE Transactions on Industrial Electronics*, vol. 53, no. 5, pp. 1398–1409, Oct. 2006, doi: 10.1109/TIE.2006.881997.
[21] W. D. Oliveira, J. P. A. Vieira, U. H. Bezerra, D. A. Martins, and B. das G. Rodrigues, "Power system security assessment for multiple contingencies using multiway decision tree," *Electric Power Systems Research*, vol. 148, pp. 264–272, Jul. 2017, doi: 10.1016/j.epsr.2017.03.029.
[22] E. Ebrahimzadeh *et al.*, "Small signal modeling of wind farms," in *2017 IEEE Energy Conversion Congress and Exposition (ECCE)*, Oct. 2017, pp. 3710–3716., doi: 10.1109/ECCE.2017.8096656.
[23] B. Shakerighadi, E. Ebrahimzadeh, F. Blaabjerg, and C. L. Bak, "Large-signal stability modeling for the grid-connected VSC based on the Lyapunov method," *Energies*, vol. 11, no. 10, Sep. 2018, doi: 10.3390/en11102533.
[24] R. Yan and T. K. Saha, "Frequency response estimation method for high wind penetration considering wind turbine frequency support functions," *IET Renewable Power Generation*, vol. 9, no. 7, pp. 775–782, Sep. 2015, doi: 10.1049/iet-rpg.2014.0364.
[25] G. Magdy, G. Shabib, A. A. Elbaset, T. Kerdphol, Y. Qudaih, and Y. Mitani, "A novel design of decentralized LFC to enhance frequency stability of egypt power system including wind farms," *International Journal on Energy Conversion (IRECON)*, vol. 6, no. 1, Jan. 2018, doi: 10.15866/irecon.v6i1.14516.
[26] F. Gonzalez-Longatt, E. Chikuni, and E. Rashayi, "Effects of the synthetic Inertia from wind power on the total system inertia after a frequency disturbance," in *2013 IEEE International Conference on Industrial Technology (ICIT)*, Feb. 2013, pp. 826–832., doi: 10.1109/ICIT.2013.6505779.
[27] L. Zhang, L. Harnefors, and H.-P. Nee, "Power-synchronization control of grid-connected voltage-source converters," *IEEE Transactions on Power Systems*, vol. 25, no. 2, pp. 809–820, May 2010, doi: 10.1109/TPWRS.2009.2032231.
[28] Q. Hu, L. Fu, F. Ma, and F. Ji, "Large signal synchronizing instability of PLL-based VSC connected to weak AC grid," *IEEE Transactions on Power Systems*, vol. 34, no. 4, pp. 3220–3229, Jul. 2019, doi: 10.1109/TPWRS.2019.2892224.
[29] J. Renedo, A. Garcia-Cerrada, and L. Rouco, "Active power control strategies for transient stability enhancement of AC/DC grids with VSC-HVDC multi-terminal systems," *IEEE Transactions on Power Systems*, vol. 31, no. 6, pp. 4595–4604, Nov. 2016, doi: 10.1109/TPWRS.2016.2517215.
[30] Y. Lu and K. Tomsovic, "Wide area hierarchical voltage control to improve security margin for systems with high wind penetration," *IEEE Transactions on Power Systems*, vol. 33, no. 6, pp. 6218–6228, Nov. 2018, doi: 10.1109/TPWRS.2018.2844281.
[31] V. S. N. Arava and L. Vanfretti, "Analyzing the static security functions of a power system dynamic security assessment toolbox," *International Journal of Electrical Power and Energy Systems*, vol. 101, pp. 323–330, Oct. 2018, doi: 10.1016/j.ijepes.2018.03.033.
[32] S. Sanchez, A. Garces, G. Bergna-Diaz, and E. Tedeschi, "Dynamics and stability of meshed multiterminal HVDC networks," *IEEE Transactions on Power Systems*, vol. 34, no. 3, pp. 1824–1833, May 2019, doi: 10.1109/TPWRS.2018.2889516.
[33] M. Supronіuk, Z. Skibko, and A. Stachno, "Diagnostics of selected parameters of electricity produced in wind power plants," *Electrotech. Rev.*, pp. 133–135, 2019, doi: 10.1002/2050-7038.12285.
[34] B. Shakerighadi, S. Peyghami, E. Ebrahimzadeh, F. Blaabjerg, and C. L. Bak, "Security analysis of power electronic-based power systems," in *IECON 2019 - 45th Annual Conference of the IEEE Industrial Electronics Society*, Oct. 2019, vol. 2019-Octob, pp. 4933–4937., doi: 10.1109/IECON.2019.8927536.
[35] S. Bahrami, M. Hadi Amini, M. Shafie-Khah, and J. P. S. Catalao, "A decentralized renewable generation management and demand response in power distribution networks," *IEEE Transactions on Sustainable Energy*, vol. 9, no. 4, pp. 1783–1797, Oct. 2018, doi: 10.1109/TSTE.2018.2815502.

BIOGRAPHIES OF AUTHORS

Hani Attar received his Ph.D. from the Department of Electrical and Electronic Engineering, University of Strathclyde, United Kingdom in 2011. Since 2011, he has been working as a researcher of electrical engineering and energy systems. Dr. Attar is now a university lecturer at Zarqa University, Jordan. His research interests include network coding, wireless sensor networks, and wireless communications. He can be contacted at email: Hattar@zu.edu.jo.

Mehrdad Ahmadi Kamarposhti received his B.Sc. degree from the Mazandaran University and M.Sc. degree from South Branch, Islamic Azad University, Tehran, Iran, in 2006 and 2008 respectively, both in electrical power engineering, and also Ph.D. degree in electrical power engineering from the Science and Research Branch, Islamic Azad University, Tehran, Iran, in 2015. He is currently an Assistant Professor with the Department of Electrical Engineering, Jouybar Branch, Islamic Azad University, Jouybar, Iran. His research interests are in FACTS devices, allocation of disturbed generation, renewable energy, optimization algorithm, microgrid, and reactive power compensation. He can be contacted at email: mehrdad.ahmadi.k@gmail.com.

Ahmed Amin Ahmed Solyman received the B.Eng. and the M.S degree in electrical and electronics engineering from MTC, Egypt, in 1999 and 2006 respectively, and a Ph.D. degree in electric and electronics engineering from the University of Strathclyde, U.K., in 2013. Currently, he is an Assistant Professor at the Department of Electrical and Electronics Engineering, Faculty of Engineering and Architecture, Nişantaşı University. His research interests include wireless communication networks, digital signal processing, IoT, bioinformatics, smart grid, and artificial intelligence. He can be contacted at email: ahmed.solyman@nisantasi.edu.tr.